Post-print of: M. Czelen, M. Rzymowski, K. Nyka and L. Kulas, "Miniaturization of ESPAR Antenna Using Low-Cost 3D Printing Process," 2020 14th European Conference on Antennas and Propagation (EuCAP), Copenhagen, Denmark, 2020, pp. 1-4, doi: 10.23919/EuCAP48036.2020.9135382.

Miniaturization of ESPAR Antenna Using Low-Cost 3D Printing Process

M. Czelen[1], M. Rzymowski[2], K. Nyka[3] *Member, IEEE* and L. Kulas[4], *Senior Member, IEEE*
Department of Microwave and Antenna Engineering,
Faculty of Electronics, Telecommunications and Informatics, Gdansk University of Technology 80-233 Gdansk, Poland,
[1] mateusz.czelen@pg.edu.pl, [2] mateusz.rzymowski@pg.edu.pl, [3] krzysztof.nyka@pg.edu.pl, [4] lukasz.kulas@pg.edu.pl

***Abstract*— In this paper, the miniaturized electronically steerable parasitic array radiator (ESPAR) antenna is presented. The size reduction was obtained by embedding its active and passive elements in polylactic acid (PLA) plastic material commonly used in low-cost 3D printing. The influence of 3D printing process imperfections on the ESPAR antenna design is investigated and a simple yet effective method to compensate them has been proposed. An antenna prototype was fabricated and measured, which showed that the experimental and simulated results are in good agreement. Realized antenna is characterized by 5.6 dBi peak gain and reflection coefficient of -17.6 dB. Base radius reduction of 23% and occupied area reduction of 40% were achieved.**

***Index Terms*—Switched-beam antenna, reconfigurable antenna, steerable antenna, electronically steerable parasitic array radiator (ESPAR) antenna, antenna miniaturization, 3D printing.**

I. Introduction

Electronically steerable parasitic array radiator (ESPAR) antenna allows one to form antenna beam and change the associated radiation direction electronically in an energy-efficient way. In typical implementation, such antennas rely on the theory introduced by Harrington [1] and have one active monopole that is surrounded by a number of passive monopoles, whose terminals are connected to variable reactances that can be controlled electronically [2].

Recently, ESPAR antennas have successfully been adopted to energy-efficient wireless sensor network (WSN) nodes operating in the 2.4 GHz industrial, scientific and medical (ISM) frequency band by connecting passive monopoles' ends to single-pole, double-throw (SPDT) switches [3], [4]. SPDT switches are used for shorting some of the monopoles to the ground, while leaving the rest of them open. It allows one to control the ESPAR antenna radiation pattern, i.e. to form the main beam and rotate it around the active monopole in the horizontal plane, using only digital input output (DIO) ports from a simple microcontroller being a part of a WSN node. In consequence, such approach enables development of cost-effective and energy-efficient WSN nodes with incorporated beam steering, localization and DoA estimation functionality to improve connectivity, coverage and energy efficiency of the whole network [5]-[7]. It can be particularly interesting for precision farming applications that require energy efficiency, big network coverage and compact size of WSN nodes [8], [9].

To reduce ESPAR antenna size so that the resulting WSN node has the most compact form, one can embed the antenna in a homogeneous dielectric material. It has been shown in [10], that using mechanically processed ceramic material having relative permittivity around 4.5 resulted in an overall footprint reduction of 50%. A similar approach could also be employed to miniaturize ESPAR antenna at lower cost using different fabrication technique, namely 3D printing. Utilization of this technology and commonly available plastic materials will also provide possibility of relatively easy and fast prototyping.

In this paper, we present the ESPAR antenna miniaturization technique by embedding its active and passive elements in polylactic acid (PLA) plastic material commonly used in low-cost 3D printing. We investigate the influence of 3D printing process imperfections on the ESPAR antenna design and propose a simple yet effective method to compensate them. We also show the measurement results of a fabricated ESPAR antenna prototype together with the achievable overall footprint reduction.

II. Antenna Concept and Design

The proposed ESPAR antenna is based on the design presented in [3]. It consist of a central active monopole surrounded by 12 parasitic elements which are mounted on a circular FR4 substrate. The monopole is fed by SMA connector, while each of the parasitic elements can be opened or shorted to the ground by its SPDT microwave switch, which makes them act as directors or reflectors, accordingly. Directional radiation pattern is obtained by setting five consecutive directors and seven reflectors. Size reduction is achieved by embedding all radiators in the cylindrical shaped dielectric overlay. The antenna structure is presented in Fig. 1.

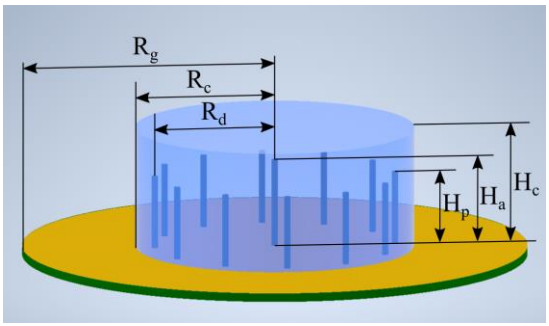

Fig. 1. Miniaturized ESPAR antenna structure

The antenna ground plane was realized as the top layer metallization of the printed circuit board (PCB), while on the bottom layer all necessary connectors, switches and electronic control circuits were placed. In order to simplify the steering circuit, the integrated SPDT FET switches NJG1681MD7 were used instead of varactor diodes [3]. Proper determination of the passive elements loading impedances significantly influences accuracy of the antenna model and design. Their values were obtained by simulating the realistic PCB layout of the switching circuit using Advanced Design System (ADS) and equal to $(26.8 - j208.5)\ \Omega$ and $(2 + j29.3)\ \Omega$ at 2.45 GHz for open and short configuration accordingly.

Electromagnetic simulation software FEKO was used to model, simulate and optimize the antenna structure. Due to its availability and low cost, the PLA filament was used to fabricate dielectric cylindrical overlay. The optimal dimensions were obtained by using a combination of Genetic Algorithm and Simplex (Nelder-Mead) algorithm. The main optimization goals were: minimization of side lobe level (SLL) maximization of antenna gain and maintaining satisfactory level of reflection coefficient. Table I compares designed miniaturized antenna dimensions with a standard-size ESPAR antenna [3]. Fig. 2 presents the simulated 3D radiation pattern.

TABLE I. MINIATURIZED ESPAR ANNTENNA DIMENSIONS COMPARED WITH STANDARD-SIZE VERSION

Dimension	Standard ESPAR antenna [3]		Miniaturized ESPAR antenna		Reduction Ratio
	$[mm]$	$[\lambda_0]$	$[mm]$	$[\lambda_0]$	
R_g	76.2	0.62	59	0.48	0.23
R_d	45	0.37	28.2	0.23	0.37
H_a	24.1	0.2	20.4	0.17	0.17
H_p	28.5	0.23	16.8	0.14	0.41
R_c	-	-	32.6	0.27	-
H_c	-	-	24.4	0.2	0.14[a]

[a] Compared to H_p of standard ESPAR antenna

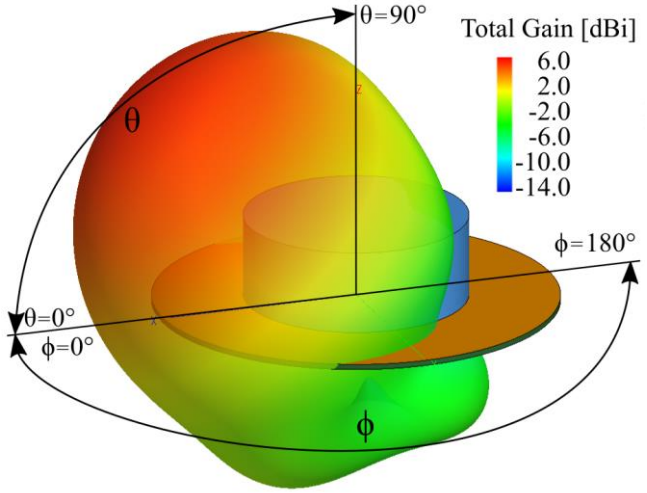

Fig. 2. Simulated 3D radiation pattern of proposed antenna at 2.45 GHz

The miniaturized antenna has 2.6 dB smaller gain, 8.6% smaller radiation efficiency and the main lobe elevation angle increased from 29° to 44° in comparison to the standard-size version. This drawback will not affect antenna usefulness, especially with respect to the DoA applications shown in [11]. The designed antenna is characterized by following parameters at center frequency: input reflection coefficient equal to -33 dB and peak gain of 5.7 dBi.

III. INFLUENCE OF 3D PRINTING PROCESS ON MINIATURIZED ESPAR ANTENNA PARAMETERS

This project is taking advantage of 3D print technology attributes such as low cost, time of production and freedom of shaping the printed object, but there are also some limitations that have to be considered. First of all, widely used and cheap materials like PLA, are not dedicated for precise RF applications, therefore the constant value of dielectric permittivity is not the manufacturer priority. As it was shown in [12] dielectric parameters also depend on the printing resolution. For this reason, their values used in this design were determined by measuring samples printed from the same spool of PLA material and with the same print settings as the desired dielectric cylinder. Obtained values are $\varepsilon_r = 2.74$ and $tan\delta = 0.01$. These values turned out to be similar to the ones measured in [13].

In this project the Fused Deposition Modeling (FDM) technique is used for 3D printing. An object is built by selectively depositing melted material in a pre-determined path layer-by-layer. Since the molten material is pressed against the previous layer, its shape is deformed to an oval. For this reason, FDM parts will always have a rippled surface. In addition, the dielectric structures needs to be printed as separated parts and then mounted on antenna. In that scenario the residual air gaps between parts is not negligible. This effect has been found to have a significant impact on presented antenna performance. The design process showed that air gaps between radiator wires and dielectric structure are crucial for antenna properties. Therefore, in order to get accurate and repetitive results, they should be deliberately introduced in the antenna design. To demonstrate their impact, a number of experiments were conducted. The air gaps dimensions, defined in Fig. 3 were swept in range from 0 to 1 mm each. Fig. 4 presents their impact on the front to back ratio in horizontal plane.

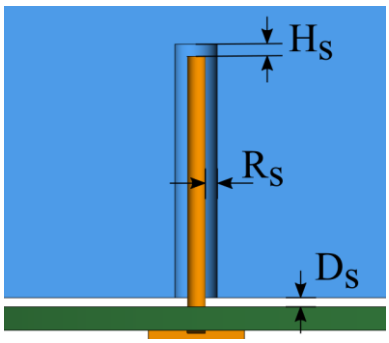

Fig. 3. Definition of the air gaps between radiator and dielectric structure dimensions

The results show that the air gap impact on the radiation pattern is significant, especially in case of the space between the dielectric and the radiator R_S. Even very narrow gaps of around 0.05 mm affect antenna performance. This is due to high electric field around radiators where even tiny air gaps cause a noticeable decrease in the effective permittivity, which eventually changes the electrical lengths of the monopole and passive elements. The experiments revealed that this effect has much smaller impact on the design for the gaps above 0.4 mm. Basing on these findings, the following air gaps dimensions were chosen for the antenna design: $H_S = R_S = 0.5$ mm and $D_S = 0.2$ mm. Fig. 5 presents impact on radiation pattern in elevation plane and Fig. 6 on the input impedance. Figures also contain results of the design optimized in presence of the air gaps.

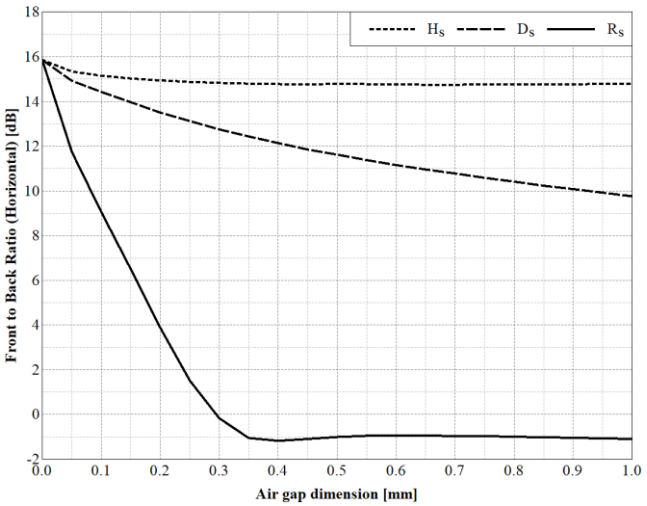

Fig. 4. Front to back ratio in horizontal plane [dB] as a function of air gaps dimensions

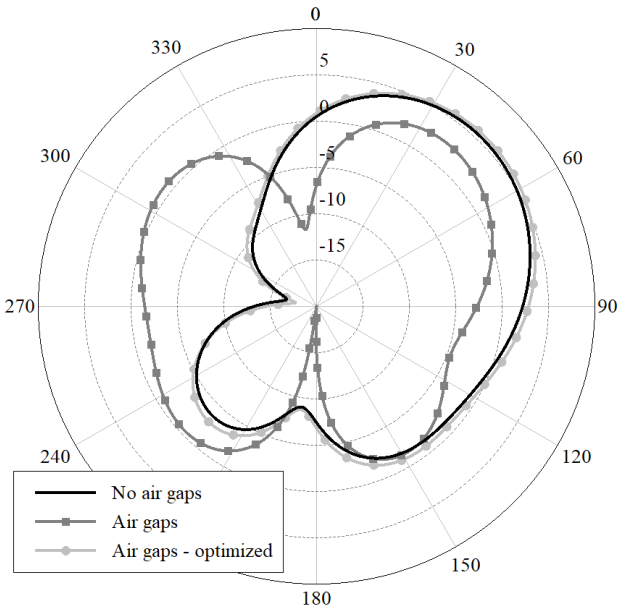

Fig. 5. Influence of the air gaps on the proposed antenna radiation pattern in elevation plane at 2.45 GHz [dBi]

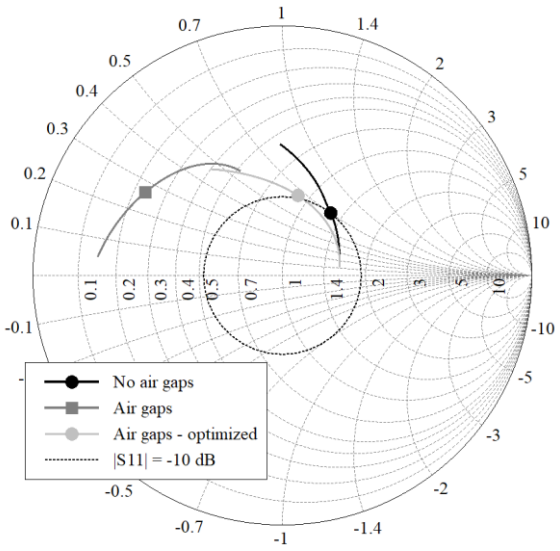

Fig. 6. Influence of the air gaps on the proposed antenna input impedance (2.3 – 2.6 GHz, marker at 2.45 GHz)

Implementing following modifications: $H_a + 1.8$ mm, $H_p + 4.6$ mm, $R_d + 2$ mm allowed to obtain similar results in terms of radiation pattern and impedance matching as in the initial design without air gap. An additional effect is the 5% efficiency increase. It has to be mentioned that the greatest dimension of antenna remains the same, so overall reduction ratio has not been affected.

IV. Measurements

In order to verify the antenna design, a prototype was fabricated and measured. Fig. 7 presents the realized prototype compared with standard-size antenna proposed in [3]. The dielectric cylinder was produced using RAISE3D Pro2 Plus printer. The simulated and measured results are similar, with respect to both, reflection coefficient (Fig. 8) and radiation pattern (Fig. 9). At the center frequency 2.45 GHz, measured antenna peak gain of 5.6 dBi and reflection coefficient values better than -17 dB have been achieved for all configurations.

In [10] the designers achieved 50% radius reduction and maximum gain of 5.1 dBi using ceramic-based material of $\varepsilon_r = 4.5$. In this work we utilized low-cost and common in 3D printing material PLA of $\varepsilon_r = 2.74$ and obtained 23% base radius reduction and peak gain of 5.6 dBi.

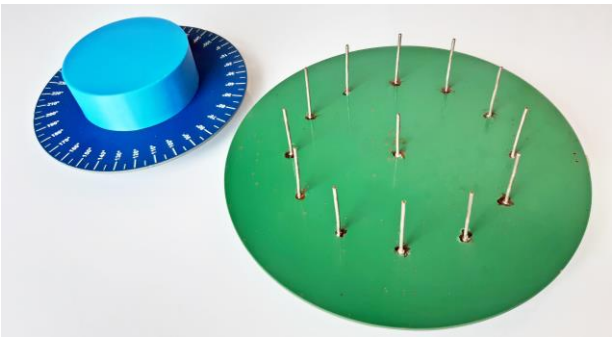

Fig. 7. Realized miniaturized ESPAR antenna compared with standard-size version [3]

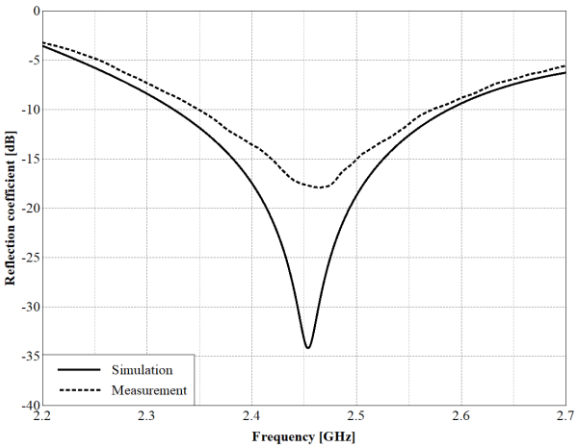

Fig. 8. Simulated and measured reflection coefficient of miniaturized ESPAR antenna [dB]

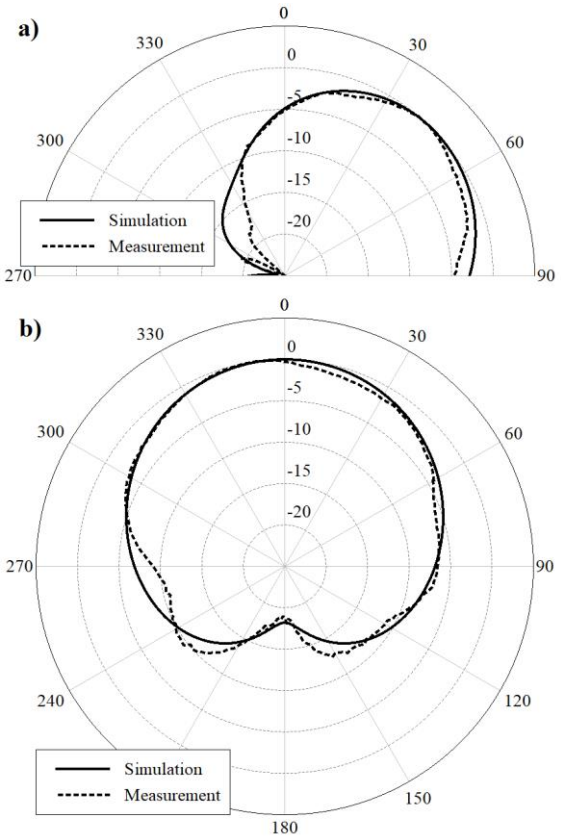

Fig. 9. Simulated and measured normalized radiation patterns of miniaturized ESPAR antenna at 2.45 GHz [dB]: a) Elevation Plane, b) Horizontal Plane

V. CONCLUSIONS

In this paper, the miniaturized version of ESPAR antenna has been presented. The concept of size reduction by embedding the monopoles in cylindrical overlay has been adopted from the literature, where the authors used mechanically processed ceramic material. This work presents the utilization of fast and low-cost 3D printing process in manufacturing of the dielectric overlay as an alternative. Using popular material PLA of $\varepsilon_r = 2.74$ allowed for 23% antenna base radius miniaturization, which corresponds to 40% occupied area reduction. Directional properties of radiation pattern and impedance matching of standard-size antenna have been maintained. The problems caused by the gaps around the monopoles have been analyzed and alleviated by introducing wider gaps in the antenna design process. In consequence, good agreement between simulated and measured results has been achieved.

ACKNOWLEDGMENT

This work was supported in part by the AFARCLOUD Project through the ECSEL Joint Undertaking (JU) under grant agreement No 783221 and in part by the European Union's Horizon 2020 research and innovation programme and Austria, Belgium, Czech Republic, Finland, Germany, Greece, Italy, Latvia, Norway, Poland, Portugal, Spain, Sweden.

The authors would like to thank the Academic Computer Centre in Gdansk, Poland (TASK) where all the calculations were carried out.

REFERENCES

[1] R. Harrington, "Reactively controlled directive arrays," *IEEE Trans. Antennas Propag.*, vol. AP-26, no. 3, pp. 390-395, May 1978.

[2] E. Taillefer, A. Hirata, and T. Ohira, "Direction-of-arrival estimation using radiation power pattern with an ESPAR antenna," *IEEE Trans. Antennas Propag.*, vol. 53, no. 2, pp. 678–684, Feb. 2005.

[3] L. Kulas, "RSS-based DoA Estimation Using ESPAR Antennas and Interpolated Radiation Patterns," *IEEE Antennas Wireless Propag. Lett.*, vol. 17, pp.25-28, 2018.

[4] M. Burtowy, M. Rzymowski, and L. Kulas, "Low-Profile ESPAR Antenna for RSS-Based DoA Estimation in IoT Applications," *IEEE Access*, vol. 7, pp. 17403-17411, 2019.

[5] M. Rzymowski, P. Woznica, and L. Kulas, "Single-Anchor Indoor Localization Using ESPAR Antenna," *IEEE Antennas Wireless Propag. Lett.*, vol. 15, pp. 1183-1186, 2016.

[6] M. Tarkowski and L. Kulas, " RSS-based DoA Estimation for ESPAR Antennas Using Support Vector Classification," *IEEE Antennas Wireless Propag. Lett.*, vol. 18, no. 4, pp. 561-565, Apr. 2019.

[7] F. Viani, L. Lizzi, M. Donelli, D. Pregnolato, G. Oliveri, and A. Massa, "Exploitation of parasitic smart antennas in wireless sensor networks," *Journal of Electromagnetic Waves and Applications*, vol. 24, no. 7, pp. 993-1003, Jan. 2010.

[8] H. Jawad, R. Nordin, S. Jawad, and M. Ismail, "Energy-efficient wireless sensor networks for precision agriculture: A review," Sensors, vol. 17, no. 8, 2017, Art. no. E1781.

[9] R. MacRuairi, M. T. Keane and G. Coleman, "A Wireless Sensor Network Application Requirements Taxonomy," *2008 Second International Conference on Sensor Technologies and Applications (sensorcomm 2008)*, Cap Esterel, 2008, pp. 209-216.

[10] Junwei Lu, D. Ireland and R. Schlub, "Dielectric embedded ESPAR (DE-ESPAR) antenna array for wireless communications," *IEEE Trans. Antennas Propag.*, vol. 53, no. 8, pp. 2437-2443, Aug. 2005.

[11] M. Rzymowski and L. Kulas, " Influence of ESPAR antenna radiation patterns shape on PPCC-based DoA estimation accuracy," *in Proc. 22nd International Microwave and Radar Conference (MIKON 2018)*, Poznan, Poland, pp. 69-72, May 2018.

[12] P. Veselý, T. Tichý, O Šefl, E. Horynová. "Evaluation of dielectric properties of 3D printed objects based on printing resolution," *IOP Conference Series: Materials Science and Engineering*, vol. 461, 2018.

[13] J. M. Felício, C. A. Fernandes, J. R. Costa, "Complex permittivity and anisotropy measurement of 3D-printed PLA at microwaves and millimeter-waves," *Proc. 22nd Int. Conf. Appl. Electromagn. Commun.*, pp. 1-6, 2016.